Numerical Modelling of Crack Path in the Contact Area of Gear Teeth Flanks

S. Glodež[1], G. Fajdiga[1] and J. Flašker[1]

[1] University of Maribor, Faculty of Mechanical Engineering, Smetanova 17, 2000 Maribor; srecko.glodez@uni-mb.si, fajdiga.gorazd@uni-mb.si, joze.flasker@uni-mb.si

ABSTRACT. *A two-dimensional computational model for simulation of contact fatigue of gear teeth flanks is presented. In the model it is assumed that the initial crack of length 0.015 mm is initiated at the surface due to previous mechanical or heat treatment of the material as well as a consequence of the running in process. The discretised model with the initial crack is then subjected to normal contact pressure, which takes into account the EHD-lubrication conditions, and tangential loading due to friction between contacting surfaces. The model considers also the moving contact of gear flanks, fluid trapped in the crack and residual stresses due to heat treatment of the material on crack propagation. The virtual crack extension method, implemented in the finite element method, is then used for simulating the fatigue crack growth from the initial crack up to the formation of the surface pit. The computational results show that the initial surface crack of length 15 μm and the considered boundary conditions lead to the appearance of very small surface pits, which can be termed as micro-pitting. The numerical results correspond well with available experimental data.*

INTRODUCTION

Two kinds of teeth damage can occur on gears under repeated loading due to fatigue, namely the pitting due to contact fatigue of gear teeth flanks and tooth breakage due to bending fatigue of gear tooth root [1]. In this paper, only the contact fatigue of gear teeth flank is addressed. Although pitting is a well-known problem in engineering and many hypotheses have been proposed to-date, the general theory to realistically and completely describe the complicated mechanism has yet to be established. The models presented in [2, 3, 4, 5] assume that gear tooth pitting may be surface or sub-surface initiated. The former is observed in gears with rough surfaces and poor lubrication, since it is strongly influenced by surface roughness and damage, like machining marks, large notches, etc. The sub-surface pitting initiation is common in gears with smooth contact surfaces and good lubrication.

The presented model for simulation of contact fatigue of gear teeth flanks is based on the theory of the short fatigue crack growth, where the crack growth rate $\mathrm{d}a/\mathrm{d}N$ is proportional to the crack tip plastic displacement δ_{pl} [6]. The purpose of this study was only the determination of the functional relationship between the stress intensity factor

K and crack length a, which is necessary to determine the crack tip plastic displacement δ_{pl} ahead of the crack and consequently crack growth rate da/dN [6]. Computational simulation of the crack growth leading to micro-pitting starts from the initial surface-breaking fatigue crack, which is a consequence of mechanical or heat treatment of the material as well as the running in process.

PARAMETERS INFLUENCING THE FATIGUE CRACK GROWTH

Normal and tangential contact loading

The normal contact pressure between meshing gear flanks has been determined using the Hertzian theory [7], where the distribution of normal contact pressure $p(x)$ can be analytically determined by (see Figure 1):

$$p(x) = \frac{2F_N}{\pi b^2}\sqrt{b^2 - x^2} \tag{1}$$

where F_N is the normal force per unit gear width and b is the half-length of the contact area, which can be determined using equivalent radius R^* and equivalent Young's modulus E^* in regard to curvature radii R_1 and R_2 in the treated point of the actual contact and Poisson rations ν_1 and ν_2 (see reference [7]). The maximum contact pressure p_0=p(x=0) can then easily be determined as

$$p_0 = \sqrt{\frac{F_N \cdot E^*}{2\pi R^*}} \tag{2}$$

The distribution of tangential contact loading $q(x)$ due to the relative sliding of the gear flanks is here determined by utilising the Coulomb friction law

$$q(x) = \mu \cdot p(x) \tag{3}$$

where μ is the coefficient of friction between the meshing gear flanks.

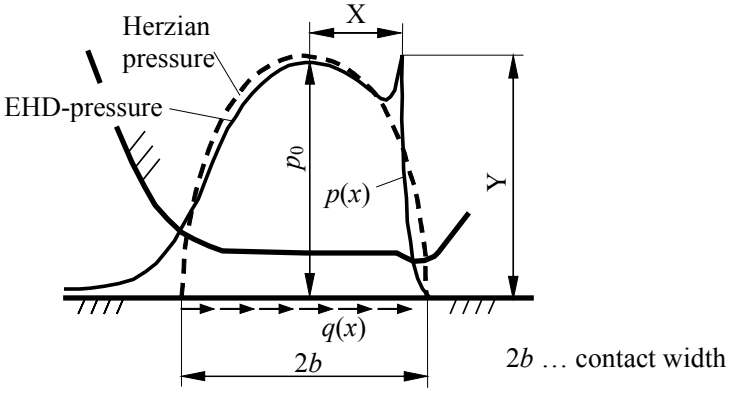

Figure 1. Loading conditions in the contact area of gear teeth flanks.

Influence of the EHD-lubrication

In the proposed computational model, the normal contact loading distribution $p(x)$ considers also the influence of the elasto-hydro-dynamic (EHD) lubrication conditions, which appear in the contact of lubricated gear flanks. In computations reported herein the dimensionless pressure spike amplitude Y and dimensionless pressure spike location X (see Figure 1) have been determined using the following empirical equations [8]:

$$Y = 0.267\, W^{-0.375}\, U^{0.174}\, G^{0.219} \tag{4}$$

$$X = 1 - 2.469\, W^{-0.941}\, U^{0.206}\, G^{-0.848} \tag{5}$$

Here, W, U and G are dimensionless parameters that are determined as follows:

- dimensionless load parameter: $$W = \frac{F_N}{E^* R^*} \tag{6}$$

- dimensionless speed parameter: $$U = \frac{\eta_o u}{E^* R^*} \quad ; \quad \eta_o = \rho \cdot \nu \tag{7}$$

- dimensionless material parameter: $$G = \alpha E^* \tag{8}$$

where η_o is the dynamic viscosity at the atmospheric pressure, $u=(u_1+u_2)/2$ is the mean surface velocity and u_1 and u_2 are respective surface velocities, ρ is the lubricant density, ν is the kinematic viscosity and α is the pressure-viscosity coefficient.

Influence of moving contact and lubricant trapped in the crack

The moving contact can be simulated with different loading configurations, as shown in Figure2. In all configurations, the normal $p(x)$ and tangential $q(x)$ contact loading are of the same magnitude, however they are acting at different positions with respect to the crack. The lubricant pressure also depends on the contact loading position.

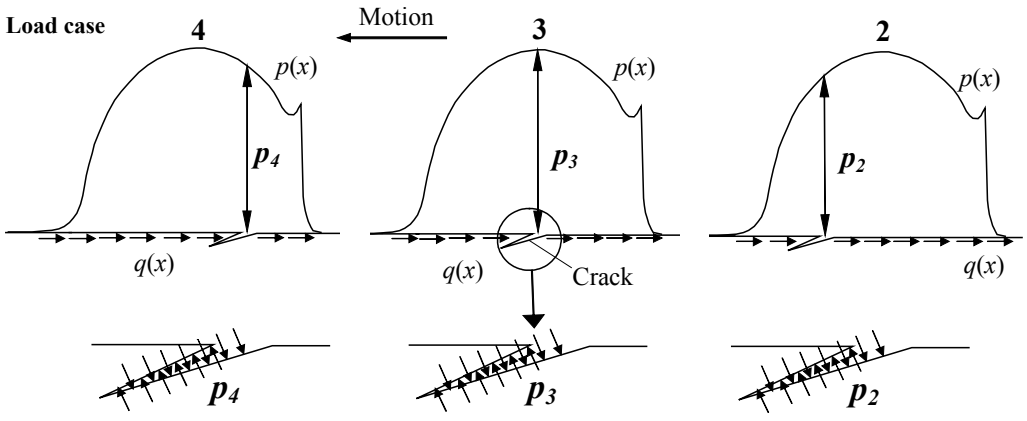

Figure 2. Different load cases and lubricant pressure acting on the crack faces

Influence of the residual stresses

To determine the residual stresses due to the heat treatment of the gear teeth flanks, the analytical model described in [9] has been used. The model is based on the hardness distribution H along the depth D under the gear flank (see Figure 3). On the basis of the hardness distribution, the carbon content C (%) in the surface layer of the gear teeth flanks can be estimated. The specific volumes of martensite, austenite and gear material before heat treatment are then a function of the carbon content. The residual stresses are assumed to be caused only by the difference in volume expansion of the material in the case and the core and can easily be estimated using the procedure described in [9].

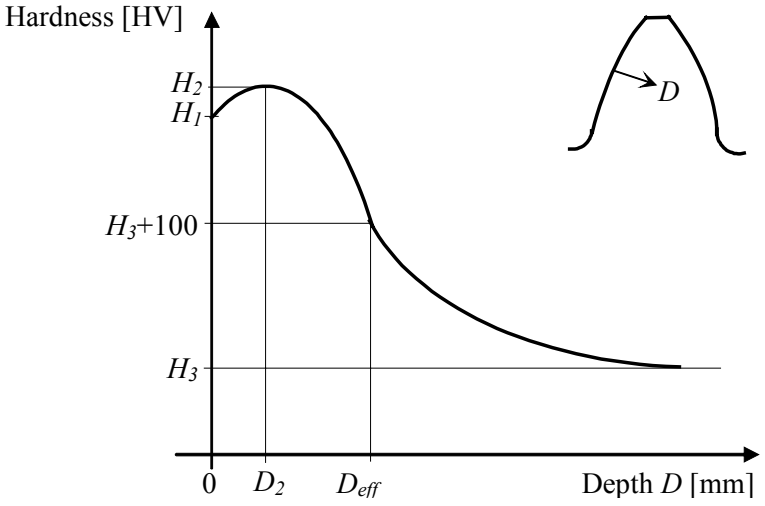

Figure 3. Hardness distribution H along depth D

NUMERICAL SIMULATION OF THE FATIGUE CRACK GROWTH

For the purpose of the fatigue crack growth simulation the virtual crack extension (VCE) method in the framework of finite element method (FEM) has been applied. The VCE method is based on the criterion of released strain energy dV per crack extension da (G =dV/da), which serves as a basis for determining the combined stress intensity factor K around the crack tip. The complete procedure for determining the stress intensity factor K using the VCE-Method is fully described in [10].

Assuming the validity of the maximum energy release criterion, the crack will propagate in the direction corresponding to the maximum value of G, *i.e.* in the direction of the maximum stress intensity factor K. The computational procedure is based on incremental crack extensions, where the size of the crack increment is prescribed in advance. For each crack extension increment, the stress intensity factor is determined in several different possible crack propagation directions and the crack is actually extended in the direction of the maximum stress intensity factor, which requires local remeshing around the new crack tip. Following the above procedure, one can numerically determine the functional relationship $K=f(a)$.

PRACTICAL EXAMPLE

The developed model has been used for simulation of the surface fatigue crack growth on a real spur gear pair, which has been experimentally tested. The gear pair is made of carburized steel 16MnCr5 (according to the ISO standard) with Young's modulus E=2.06·10^5 N/mm^2 and Poisson ratio ν=0.3. The maximum contact pressure p_0=1550 N/mm^2 is acting at the inner point of single teeth pair engagement (point B), with the equivalent radius of gear teeth flanks R^*=10 mm and half-length of the contact area b=0,274 mm. The Hertzian normal loading distribution $p(x)$ along the entire contact width of the gear flanks has then been determined using eq. (1).

For all computations, the coefficient of friction μ=0.04 has been used, which is the average value for well-lubricated gears [11]. Therefore, the tangential loading $q(x)$ has been determined using eq. (3).

The influence of EHD-lubrication on the normal loading distribution $p(x)$ has been estimated using eqs. (4) to (8) for the lubricant oil ISO-VG-220, with the kinematic viscosity ν_{40} = 220 mm^2/s, density ρ_{15} = 0.9 kg/dm^3 and pressure-viscosity coefficient α=0.18·10^{-7} m^2/N. The mean surface velocity of the contacting surfaces has been taken as a constant value u=5 m/s, which is a common value for gears [11]. Using these parameters, the dimensionless pressure spike amplitude Y and the dimensionless pressure spike location X (see Figure 1) are equal to X= 0.9462 and Y= 0.8146, respectively.

The hardness distribution H and the carbon content C (%) in the surface layer of the gear teeth flanks have been determined using the theory described in [9], where the following values have been measured previously: H_1=765 HV, H_2=770 HV, H_3=450 HV, D_{eff} =1.25 mm, D_2 =0.1 mm (see Figure 3). The distribution of residual stresses on the basis of hardness distribution is shown in Figure 4.

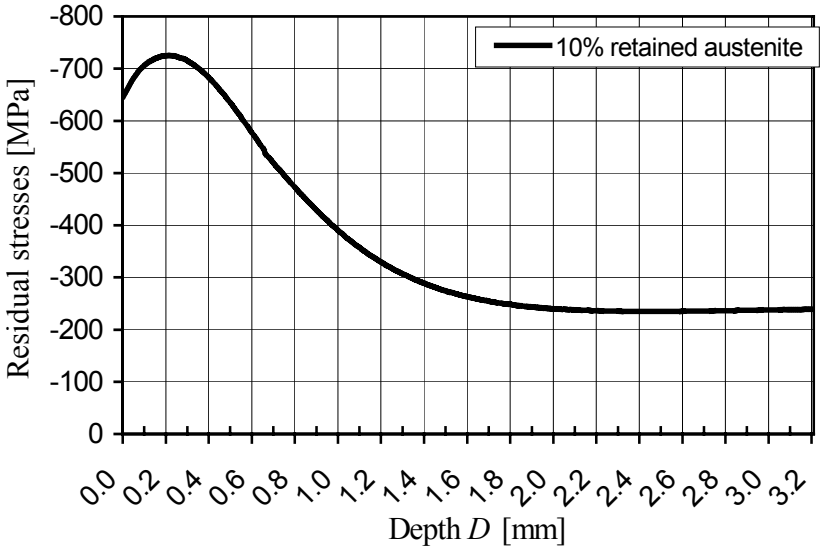

Figure 4. Distribution of the residual stresses along depth D

Numerical calculations

The finite element mesh shown in Figure 5, and the boundary conditions as described above, have been used in subsequent analyses. For the configuration of the initial crack on the surface, located at point B, it was assumed that the initial length of the crack is equal to a_o=15 μm, with the initial inclination angle towards the contact surface equal to α_o = 22°. It is recognized, that the predicted crack growth heavily depends on the size and orientation of the initial crack. However, the used configuration follows the metallographic investigations of initial cracks appearing on similar gears [12].

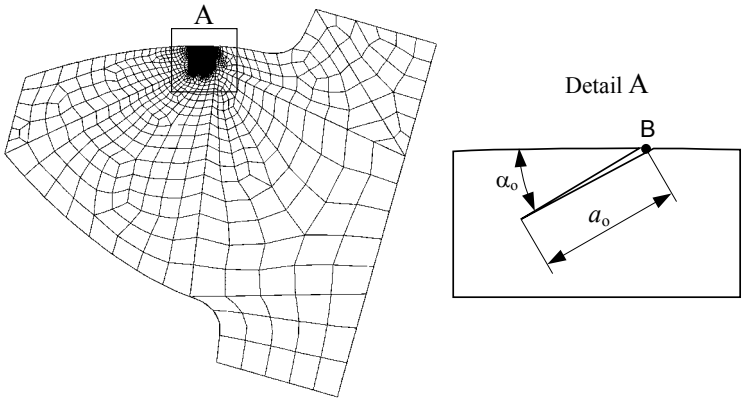

Figure 5. FE discretisation and configuration of the initial crack

In this study, the virtual crack extension method implemented in the finite element method has been used for computational estimation of the stress intensity factor K and subsequent incremental crack growth simulation. In numerical computations, the crack increment was of size Δa = 1.5 μm. The stress intensity factor K was estimated in each crack increment for 30 different virtual crack tip extensions. Five different loading configurations have been considered in each computation for the purpose of simulating the effect of the moving contact of the gear flanks (see Figure 2). For each crack increment, the crack was actually extended in the direction of the recorded K_{max} from all calculated load cases. It can be seen that the computed stress intensity factor K is very small at the beginning, but later increases as the crack propagates towards the contact surface. Numerical simulations have shown that at the moment when the crack reaches the vicinity of the contact surface, the stress intensity factor is extremely high. At that moment it can be expected that the material surface layer breaks away and the pit occurs on the surface (Figure 6 - step 1). Because of the very small dimensions of surface pits, they can be termed micro pitting.

Micro pitting as shown in (Figure 6 - step 1) is not the final failure. Further operation of the gear pair results in the formation of larger pits. In this respect, similar numerical simulations have been continued for two more steps (Figure 6). In these calculations, it was assumed that the initial crack a_o=7.5 μm started from the bottom of the existing surface pit. The results show that the compressive residual stresses have a conservative influence on the crack propagation, because the stress intensity factor K is lower when compared to the results without residual stresses.

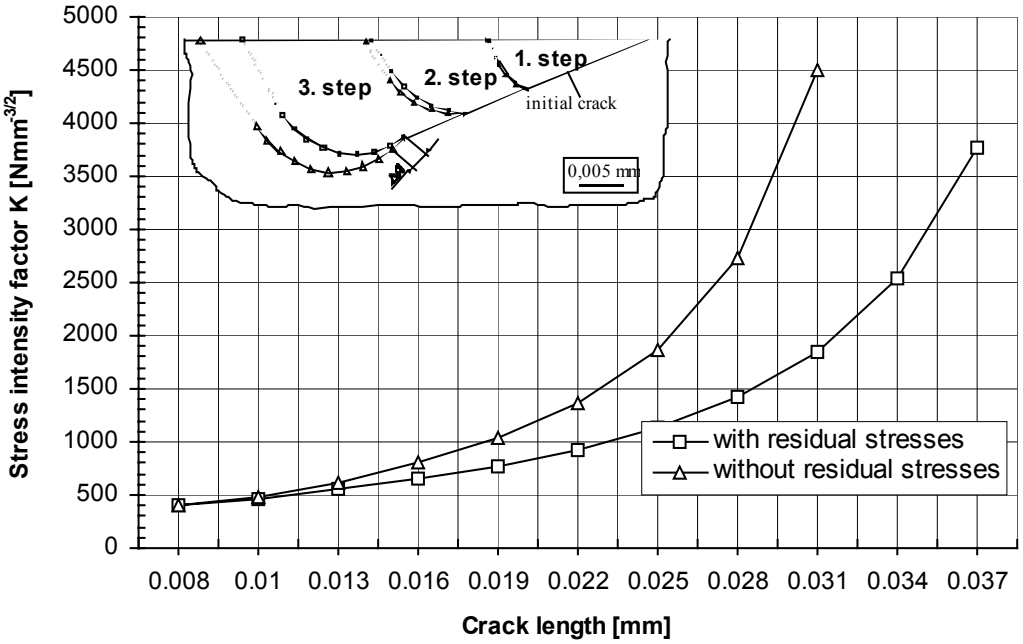

Figure 6. Maximum SIF for crack propagation from the existing micro pit

Experimental testing

Experimental testing of the spur gear pair has been performed on a FZG- pitting test machine according to the DIN 51354 standard. The tested gears have been subjected to the same operating conditions and loading parameters as used in the numerical computations. Figure 7 shows the comparison between numerically and experimentally determined pits on the gear flanks.

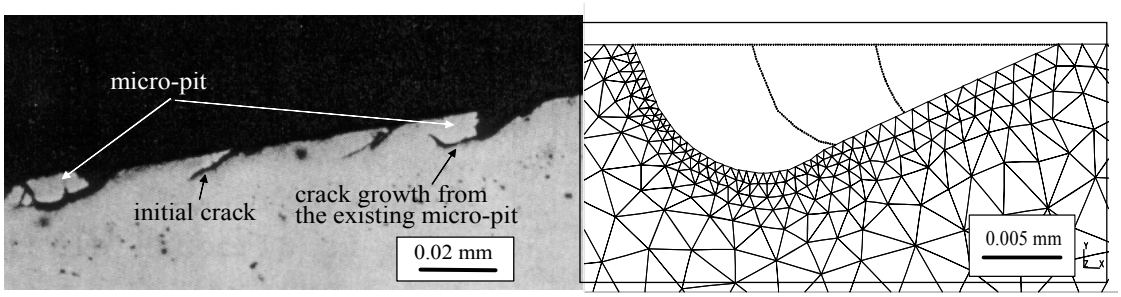

Figure 7. Experimentally (left) and numerically (right) determined pit shapes

CONCLUSIONS

The paper presents a computational model for the simulation of surface initiated fatigue crack growth on gear teeth flanks. A simple contact model is used for simulating fatigue crack growth under conditions of rolling and sliding contact. The contact model is subjected to moving normal (normal contact pressure) and tangential (frictional forces) contact forces, which also take into account the influence of EHD-lubrication

conditions, the associated lubricant pressure acting on the crack faces, and residual stresses due to the heat treatment of the gear material. Here, the effect of lubricant pressure within the crack is very important because it refers to Mode I crack opening. Therefore, the Mode II opening and crack closure can be neglected. During numerical simulations it was assumed that the lubricant pressure is constant along the whole crack length for each load case, although it is probably not the case in real gear operation.

On the basis of the results in Figures 6 and 7, it can be concluded that the initial surface crack of length 15 μm with the considered boundary conditions led to the appearance of very small surface pits, which can be termed *micro-pitting* on the gear teeth flanks. However, the presented model enables the simulation of further growth of such a micro-pit on the surface. If the numerical procedure as shown in Figure 7 would be continued, the surface pits would become larger and larger, and after some period of time they would attain the dimensions of classical pitting or spalling.

The computational determination of the functional relationship $K = f(a)$ from Figure 6 enables an estimation of the service life of gears with regard to micro-pitting, if combined with the model developed previously in [4, 11]. In addition, the model can be further improved as additional contributions from theoretical and numerical research become available, coupled with new data from more refined experimentation.

REFERENCES

[1] ISO 6336 (1993), Calculation of Load Capacity of Spur and Helical Gears, International Standard.

[2] G. R. Miller, L. M. Keer and H. S. Cheng (1985) On the mechanics of fatigue crack growth due to contact loading, *Proc. Roy. Soc. London*, **A397**, 197-209.

[3] R. S. Zhou, H. S. Cheng and T. Mura (1989) Micropitting in Rolling and sliding contact under mixed lubrication, *ASME J. Tribology*, **111**, 605-613.

[4] S. Glodež, H. Winter and H.P. Stüwe (1997) A fracture mechanics model for the wear of gear flanks by pitting, *Wear*, **208**, 177-183.

[5] D.I. Fletcher and J.H. Beynon (2000) The effect of contact load reduction on the fatigue life of pearlitic rail steel in lubricated rolling-sliding contact, *Fatigue Fract Engng Mater Struct*, **23**, 639-650.

[6] Z. Sun, E. R. de los Rios and K. J. Miller (1991),Modelling small fatigue cracks interacting with grain boundaries, *Fatigue Fract. Engng Mater. Struct.*, **14**, 277-291.

[7] K. L. Johnson (1985) *Contact mechanics*. Cambridge University Press.

[8] B.J. Hamrock, R.T. Lee, L.G. Houpert (1987) Parametric study of performance in elastohydrodynamic lubricated line contact, *Fluid film lubrication–Osborne Reynolds centenary*, 199-206.

[9] T. Tobe, M. Kato, K. Inoue, N Takatsu and I. Morita (1986) Bending Strength of Carburized SCM42OH Spur gear Teeth , *JSME*, **29**, 273-280.

[10] T. K. Hellen (1975) On the method of virtual crack extensions, *International Journal for Numerical Methods in Engineering*, **9**, 187-207.

[11] S. Glodež (1996) *The fracture mechanics model of gear flanks fatigue*, Ph.D thesis, Faculty of Mechanical Engineering, University of Maribor.

[12] G. Knauer (1988) *Zur Grübchentragfähigkeit einsatzgehärteter Zahnräder*, Ph.D. thesis, TU Munich, 1988.